View Article Online
View Journal

Green Chemistry

Cutting-edge research for a greener sustainable future

Accepted Manuscript

This article can be cited before page numbers have been issued, to do this please use: A. J. Shapiro, R. C. O'Halloran, D. Tavares, D. Huynh, S. Han, R. Shi, Y. Gupta, R. M. O'Dea, S. Haney, Y. Otsuka, S. Sadula, D. G. Vlachos, M. Ierapetritou, D. F. Levia and T. Epps, III, *Green Chem.*, 2026, DOI: 10.1039/D6GC01047D.

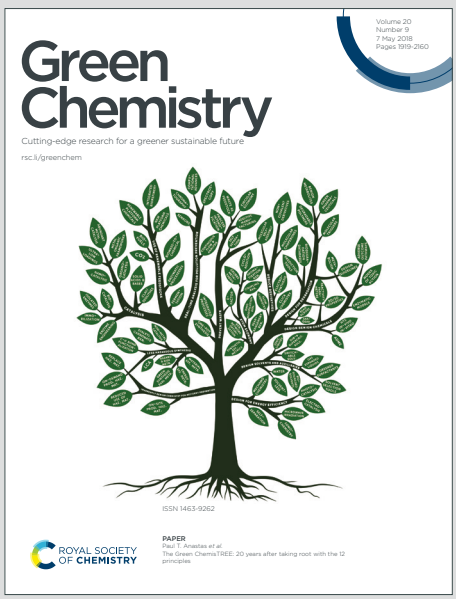

This is an Accepted Manuscript, which has been through the Royal Society of Chemistry peer review process and has been accepted for publication.

Accepted Manuscripts are published online shortly after acceptance, before technical editing, formatting and proof reading. Using this free service, authors can make their results available to the community, in citable form, before we publish the edited article. We will replace this Accepted Manuscript with the edited and formatted Advance Article as soon as it is available.

You can find more information about Accepted Manuscripts in the Information for Authors.

Please note that technical editing may introduce minor changes to the text and/or graphics, which may alter content. The journal's standard Terms & Conditions and the Ethical guidelines still apply. In no event shall the Royal Society of Chemistry be held responsible for any errors or omissions in this Accepted Manuscript or any consequences arising from the use of any information it contains.

View Article Online
DOI: 10.1039/D6GC01047D

View Article Online
DOI: 10.1039/D6GC01047D

1. This work highlights the potential of forestry residues as profitable and sustainable biorefinery feedstocks to address global environmental, social, and resource security concerns associated with our current fossil fuels-based economy. We conducted techno-economic analysis (TEA) and life cycle assessment (LCA) for a model integrated reductive catalytic fractionation (RCF)-molten salt hydrolysis biorefinery using forestry residues differing in species, tree part, and phenophase as feedstocks.
2. We demonstrated that through optimized feedstock selection, approximately 4x and 8x reductions in greenhouse gas emissions and phenolic minimum selling prices can be achieved, respectively. Furthermore, we identified biomass with high RCF yields and hemicellulose contents as optimal feedstocks.
3. TEA and LCA revealed emission and cost drivers, such as the RCF reactor pressure. Future research on these key parts of the process can improve the overall biorefinery sustainability.

View Article Online
DOI: 10.1039/D6GC01047D

Forest residue harvest optimization: Spanning the bridge between plant biology and biorefinery performance

Alison J. Shapiro[1#], Robyn C. O'Halloran[2#], Devin Tavares[1#], Dat Huynh[1], Seulki Han[1], Ruofan Shi[1], Yagya Gupta[1,3], Robert M. O'Dea[1,4], Sara G. Haney[5], Yuichiro Otsuka[6], Sunitha Sadula[3], Dionisios G. Vlachos[1,3], Marianthi Ierapetritou[1], Delphis F. Levia[2,7,8*], Thomas H. Epps, III[1,9,10*]

[1] Dept. of Chemical & Biomolecular Engineering, University of Delaware, Newark, DE, 19716 USA
[2] Dept. of Civil, Construction, and Environmental Engineering, University of Delaware, Newark, DE, 19716 USA
[3] Catalysis Center for Energy Innovation, RAPID Manufacturing Institute & Delaware Energy Institute, University of Delaware, Newark, DE, 19716 USA
[4] Center for Plastics Innovation (CPI), University of Delaware, Newark, DE, 19716 USA
[5] Dept. of Chemistry & Biochemistry, University of Delaware, Newark, DE, 19716 USA
[6] Dept. of Forest Resource Chemistry, Forestry and Forest Products Research Institute, Tsukuba, Ibaraki 305-8687, Japan
[7] Dept. of Geography & Spatial Sciences, University of Delaware, Newark, DE, 19716 USA
[8] Dept. of Plant & Soil Sciences, University of Delaware, Newark, DE, 19716 USA
[9] Dept. of Materials Science & Engineering, University of Delaware, Newark, DE, 19716, USA
[10] Center for Research in Soft matter and Polymers (CRiSP), University of Delaware, Newark, DE, 19716 USA

[#]These authors contributed equally to this work.
*Corresponding authors: thepps@udel.edu, dlevia@udel.edu

View Article Online
DOI: 10.1039/D6GC01047D

Abstract

Forestry residues have immense potential as alternative feedstocks to petroleum, yet their inherent complexity remains a major challenge to widespread use. Pairing temporal rhythms of plant biology with biorefinery performance is critical to industrial-scale biorefinery development. Here, we provide the first report of a techno-economic analysis (TEA) and life cycle assessment (LCA) for a model integrated reductive catalytic fractionation (RCF)-molten salt hydrolysis process for forestry residues varying in tree part, species, and phenophase. All forestry residues resulted in net-negative greenhouse gas (GHG) emissions vs. comparable petroleum feedstocks, with GHG emissions potentially reduced >4.0x through composition-based feedstock selection (*e.g.,* harvesting American beech bark in spring vs. summer). Moreover, American beech twigs/branchlets and bark in leafed and emergence phenophases, respectively, had 7.9x lower predicted phenolic minimum selling prices (MSPs) vs. other feedstocks and MSPs within the current global phenolic market range. Hemicellulose content and RCF yield emerged as key parameters impacting GHG emissions and biorefinery revenue, identifying hardwood twigs/branchlets in the leafed phenophase as optimal biofeedstocks. Biorefinery expenses were dominated by purchased equipment, raw materials, and utility costs, highlighting essential areas for future study. Notably, RCF reactor pressures drove 85-90% of equipment costs, but sensitivity analysis revealed that decreasing the pressure 20% could reduce the phenol MSP 4-fold. Structural carbohydrate dynamics were also investigated using a two-step acid hydrolysis method to resolve tissue- and species-level patterns in biomass composition throughout the year to enable harvest optimization based on TEA/LCA findings. Ultimately, elucidating the impact of biofeedstock dynamics on biorefinery performance enables harvest optimization, informed engineering design, and progress towards an expanded bioeconomy.

View Article Online
DOI: 10.1039/D6GC01047D

Introduction

Lignocellulosic biomass is a vast renewable resource with tremendous potential as a fossil fuel alternative to address global resource scarcity and sustainability challenges.(1-4) Lignocellulosic biomass-derived products have the potential to significantly reduce environmental impacts relative to petroleum-derived products by mitigating GHG emissions and generating socioeconomic benefits.(5) Unlike first-generation biofeedstocks (*i.e.,* food crops), this resource does not compete with food production or occupy arable land, making it an attractive feedstock for biorefineries.(6) Forestry residues and other underutilized lignocellulosic sources are particularly promising because they are available in enormous quantities, at low costs, and with minimal additional environmental impact.(7-9) In the U.S. in 2023, ~30 million dry tons of forestry residues were estimated to be available in the near term, with up to 63 million dry tons potentially available in a mature market scenario at $40-70/dry ton.(10) Despite their availability and potential for valorization, most of these residues are burned for energy generation or left in forests.(11) A major challenge to employing these residues as biorefinery feedstocks is their structural complexity and compositional diversity.(4, 7) Thus, there is a significant need to predict biofeedstock structural complexity and understand its economic and environmental impact to inform feedstock selection, inventory management, and processing conditions to enable profitable and sustainable industrial biorefineries.

Structural carbohydrates, such as cellulose and hemicellulose, typically constitute >50% of biomass dry weight and form the rigid framework of plant cell walls.(12-14) Cellulose is a semi-crystalline glucose polymer with degrees of polymerization reaching up to ~10,000 units, whereas hemicellulose is an amorphous, heterogeneous polymer composed of mixed hexose and pentose sugars with degrees of polymerization of ~50–300 units.(13, 14) The cell wall microstructure and strength are strongly influenced by cellulose crystallinity, hemicellulose branching, and carbohydrate composition.(15, 16) These structural features impact the overall efficiency of biomass fractionation and deconstruction; therefore, understanding how carbohydrate composition varies across species and residue types is critical for anticipating biorefinery performance.(17-19) Furthermore, several studies have now demonstrated that lignin (*i.e.,* the aromatic, heterogeneous network comprising >40 wt% in forestry residues (20)) also must be valorized for biorefineries to achieve commercial viability without inhibiting the efficiency of sugar liberation during deconstruction.(21-23) Lignin-first biorefinery strategies address part of this challenge by extracting and stabilizing lignin early in processing to mitigate the production of more recalcitrant lignins.(13) Reductive catalytic fractionation (RCF) is the most common such approach and uses a hydrogen donor and metal catalyst to solvate, depolymerize, and stabilize lignin.(13) Molten-salt-hydrate (MSH) saccharification provides a complementary route for cellulose-rich streams by efficiently liberating sugars under mild conditions relative to other carbohydrate hydrolysis strategies that require concentrated acids and/or high temperatures.(24-27) Mechanistic studies have revealed that selective and efficient deconstruction in the MSH catalytic system originates from strong interactions between the Lewis acidic metal ion (Li^+) and coordinated water molecules, disrupting both intra- and intermolecular hydrogen bonding and resulting in high sugar yields from structural carbohydrates while separating <95% pure lignin as solids.(26, 28, 29) In combination, an integrated RCF–MSH biorefinery can efficiently convert forestry residues into valuable products – including *p*-xylene and furfural from structural carbohydrates and phenolics from lignin. Global markets are valued at ~$13 billion (2023) for *p*-xylene and ~$440 million (2021) for furfural.(30, 31) Although the majority of the current commercial *p*-xylene is fossil fuel-based, the current global market size

View Article Online
DOI: 10.1039/D6GC01047D

of biobased *p*-xylene is valued at $615 million (2024) and is anticipated to continue growing.(32) Phenolic products also show promise as precursors for biobased lubricants, polymers, additives, cosmetics, and pharmaceuticals.(33-37) Literature indicates that the production of *p*-xylene, furfural, and phenolics from forestry residues can achieve a net-negative global warming potential relative to petrochemical alternatives,(38) yet the economics and the influence of species-, phenophase- and residue-specific carbohydrate and lignin composition on integrated RCF-MSH performance remains largely unexplored. Quantification of the impacts of variations in structural carbohydrate and lignin composition, abundance, and dynamics can inform process optimization and guide feedstock selection for improved biorefinery outcomes.

In this study, we evaluated the biomass composition of forestry residues, namely bark, twigs/branchlets, and foliage, across four species and phenophases to capture full-year variation relevant to biorefinery performance. This year-round dataset enabled realistic integration of feedstock variability into downstream process modeling. For the first time, we directly connected forestry residue biofeedstock dynamics to biorefinery economics and environmental impacts to understand how biomass composition shapes biorefinery performance. We conducted a techno-economic analysis (TEA) and life cycle assessment (LCA) for forestry residues in an RCF-MSH integrated lignocellulosic biorefinery to produce *p*-xylene, furfural, and phenols. Comparison of forestry residues across tree part, phenophase, and species highlighted how biorefinery outputs, economics, and greenhouse gas (GHG) emissions are dictated by feedstock selection. For instance, furfural yields were 91% higher in the scenario in which twigs/branchlets were used vs. bark for the same species and time of year (*i.e.,* American beech in the leafless phenophase) because of the difference in hemicellulose quantities between residues. As hemicellulose content and RCF yields were the biomass composition components that most significantly impacted GHG emissions and biorefinery revenue, we proposed that forestry residue harvesting should be optimized to maximize the valorization of twigs/branchlets from hardwood trees in the leafed phenophase. Furthermore, we identified major drivers for biorefinery costs as purchased equipment, raw materials, and utilities, for which the RCF reactor (pressure), biomass drying/transportation & LiBr, and steam were the dominant contributors, respectively. We discuss key areas of current and future research for biorefinery development to reduce these expenses and ultimately increase the economic viability of commercial biorefineries. Overall, this study bridges the gap between plant biology and biorefinery performance, highlighting the immense potential of forestry residues as profitable and sustainable biofeedstocks.

View Article Online
DOI: 10.1039/D6GC01047D

Results and Discussion

Elucidating the dynamics of structural carbohydrates

Forestry residues (bark, twigs/branchlets, foliage) were collected for four species native to the Eastern U.S. (American beech, sweet birch, pitch pine, yellow poplar) in each of the four canopy phenophases (senescence, leafless, emergence, leafed). Structural carbohydrates were analyzed in dry, extractive-free residues using a two-step acid hydrolysis procedure to quantify the sugars *via* high-performance liquid chromatography (HPLC).(39) Fig. 1 shows glucan (cellulose), xylan (assumed to be the primary component in forestry residue hemicellulose),(38, 40-43) and total structural sugars (reported as the sum of glucan and xylan) grouped by species and residue. Tabulated biomass compositional data can be found in Tables S1 and S2.

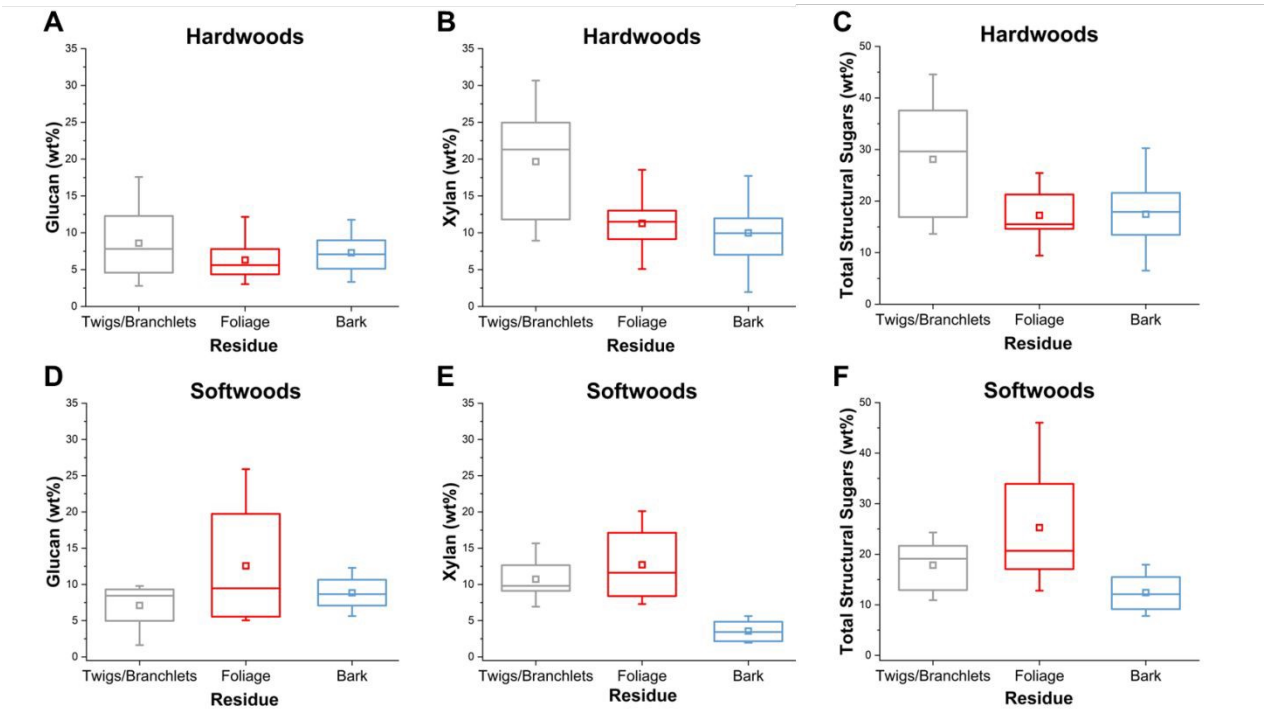

Fig. 1. Structural carbohydrate contents grouped by hardwoods and softwoods. Glucan, xylan, and total structural sugars for A-C) Hardwoods (American beech, sweet birch, and yellow poplar) and D-F) Softwoods (pitch pine) for twigs/branchlets, foliage, and bark. Total structural sugars are the sum of glucan and xylan. The box indicates the interquartile range of the data, spanning from the first to the third quartile. The whiskers indicate the minimum and maximum data points, the square within the box denotes the mean, and the horizontal line inside represents the median (50th percentile). For all hardwood twigs/branchlets and bark, $n = 24$, for hardwood foliage, $n = 18$, and for all softwood tree parts, $n = 8$. Values are reported on a dry, extractive-free basis.

Twigs consistently had the highest median structural sugar concentrations in hardwoods, likely because this woody tissue tends to be dominated by cellulose and hemicellulose.(38, 44) Bark, in contrast, had lower and more variable sugar content. This finding aligns with previous studies noting its higher proportions of lignin, suberin, and extractives.(20, 45) Foliage showed the greatest

View Article Online
DOI: 10.1039/D6GC01047D

variability, most likely reflecting fluctuations in carbohydrate pools that are driven by phenology and species-specific differences in photosynthetic activity, storage, and sugar export,(46) with softwoods exhibiting the highest foliage structural sugar concentrations overall. Across species, structural carbohydrates also followed broad phenophase patterns: bark and twigs showed higher glucan and xylan values during the leafed and leafless phenophases and lower values during emergence and senescence, whereas foliage structural sugar content peaked in the leafed phenophase and declined in senescence and leafless. Distinct differences were observed between softwood (pitch pine) and hardwood species (American beech, sweet birch, yellow poplar; Fig. 1). For both twigs/branchlets and bark, the median xylan content was significantly different ($p_{twigs} = 0.013$, $p_{bark} = 0.020$) between hardwoods and softwoods. Foliage in pitch pine was more variable and generally higher than hardwoods throughout the year. Within hardwood species, yellow poplar had the highest sugar concentrations across tissues, and American beech had the lowest. In twigs/branchlets across all species, xylan varied significantly ($p = 0.015$), suggesting that xylan drives the differences between species. This finding is consistent with the species-level differences observed in these woody tissues; differences in secondary cell wall composition have been reported among species – hardwoods typically contain higher proportions of xylan-rich hemicellulose.(47) Tabulated statistical data are shown in Tables S3-S5, and additional structural carbohydrate plots are shown in Figs. S1-S3.

Connecting feedstock selection to biorefinery performance

Beyond understanding the dynamics of the forestry residues themselves, it is critical to connect how changes in feedstock impact overall biorefinery economics and environmental impacts. A process model for an integrated RCF-MSH biorefinery was adapted from literature(38) and used as the basis for the TEA and LCA. Herein, for the first time, phenophase, species, and tissue type are taken into account to conduct both an LCA and a TEA. Forestry residues were assumed to contain the following components: cellulose, hemicellulose, lignin, extractives, and ash. The cellulose and hemicellulose data were those reported in the previous section. The lignin, ash, and extractive contents and the RCF phenolic yields used in the process model were taken from previous work.(20) For more details on the model, inputs (Table S6), and assumptions, see the Experimental Methods and SI Section 3. The biorefinery model (Fig. 2) consists of three steps. In the first step, RCF converts lignin to phenolics but leaves the structural carbohydrate fraction intact. The RCF reactor was loaded with methanol, hydrogen gas, and a 5 wt% Ru/C catalyst, and operated at 80 bar and 250 °C. After separations and cooling steps, the unreacted biomass entered the second step of the process, MSH, which converts cellulose and hemicellulose into *p*-xylene and furfural. In this step, LiBr breaks down cellulose and hemicellulose, which are then converted to hydroxymethylfurfural (HMF) and furfural in a biphasic reactor and separated. The HMF undergoes hydrodeoxygenation and cycloaddition reactions to produce *p*-xylene, which is then purified. Unreacted lignin and humin byproducts then enter step three of the process, steam and power generation (STP), which burns them to generate the electricity and steam used in the biorefinery. Phenols, *p*-xylene, and furfural were chosen as the biorefinery outputs to maximize the whole biomass valorization by generating valuable products from all three primary components of the forestry residues (lignin, cellulose, and hemicellulose, respectively).

View Article Online
DOI: 10.1039/D6GC01047D

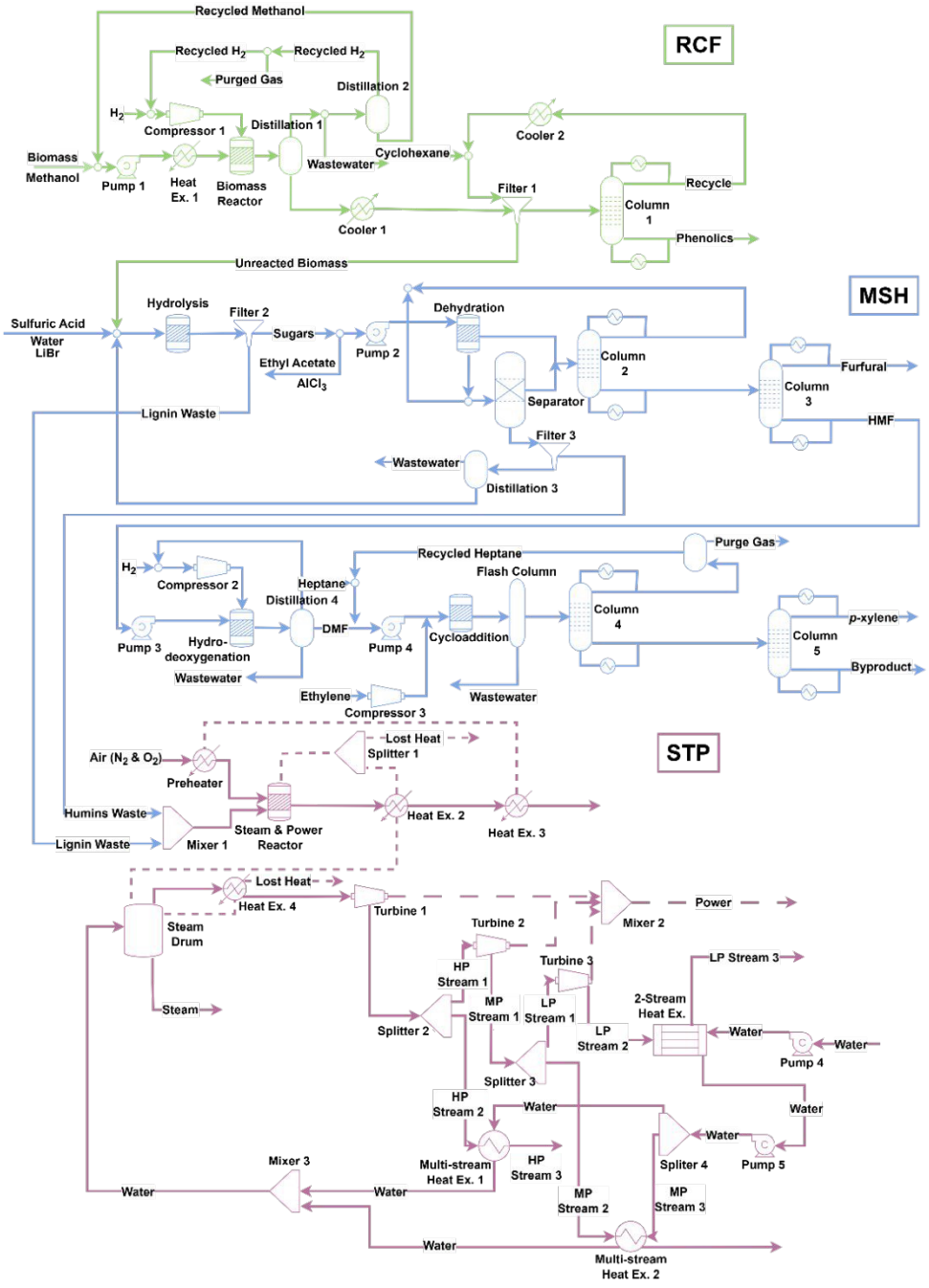

Fig. 2. Process overview diagram of modeled biorefinery. Biomass enters the biorefinery, in which lignin is fractionated and deconstructed in the RCF process (green) to produce phenols. The unreacted biomass from the RCF enters the MSH process (blue), which hydrolyzes and dehydrates the sugars to produce furfural and *p*-xylene. The lignin and humin waste enter the STP (purple), in which they are burned to reduce overall energy use for the biorefinery. LP, MP, and HP stand for low, medium, and high pressure, respectively. HMF and DMF are 5-hydroxymethylfurfural and dimethylformamide, respectively. Solid lines represent material flows, and dashed lines represent heat/power flows.

View Article Online
DOI: 10.1039/D6GC01047D

A representative sample set of nine forestry residues showing variation in phenophase, species, and tree part was used in the process model to elucidate how feedstock selection impacts overall biorefinery outputs (Fig. 3). These nine residues were chosen to have a complete set of each of the four species, four phenophases, and three tree parts. Furthermore, this representative set enables isolated comparison of the impact of each parameter (*e.g.,* American beech bark can be evaluated in each phenophase). There are substantial differences in composition and RCF phenolic monomer yield across the nine residues, enabling the identification of the impact of feedstock composition on overall biorefinery performance. In just one example, furfural yields (expressed in %change relative to the lower output) can increase by 91% by choosing American beech leafless twigs/branchlets over American beech leafless bark, 76% by choosing leafless American beech bark over leafed-winter (W) pitch pine bark, or 88% by choosing the American beech bark in the leafless over American beech bark in the leafed phenophase. Hemicellulose content largely drives these significant differences in biorefinery product output. In another example, biorefinery phenolic outputs are significantly higher in American beech bark in the leafed phenophase, relative to all other phenophases, due to the large differences in phenolic monomer yields between these phenophases.

View Article Online
DOI: 10.1039/D6GC01047D

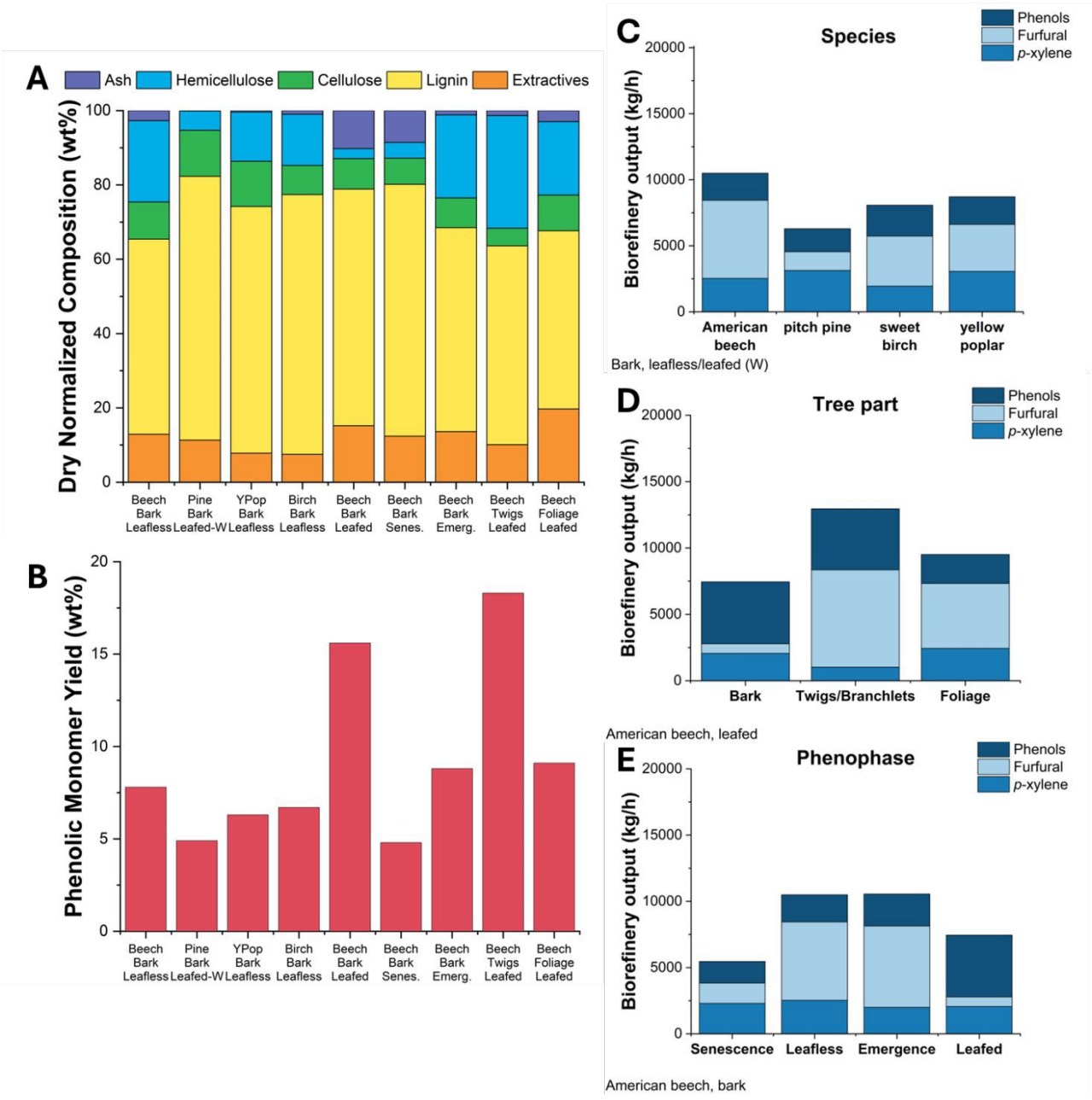

Fig. 3. Model forest residue biorefinery inputs and outputs. A) Difference in composition between biorefinery inputs, B) differences in phenolic monomer yield between biorefinery inputs, C) differences in biorefinery output grouped by species, D) differences in biorefinery output grouped by tree part, and E) differences in output grouped by phenophase. Tree part samples are for American beech in the leafed phenophase; species samples are for bark during the leafless (leafed-W for pitch pine) phenophase; and phenophase samples are for American beech bark. YPop is yellow poplar; senes. is senescence; and emerg. is emergence.

View Article Online
DOI: 10.1039/D6GC01047D

Techno-economic analysis

TEA is a holistic framework that encompasses various economic evaluation approaches, and different economic metrics may be applied depending on the study objective. Herein, a TEA was conducted to identify the impact of biomass compositional dynamics on biorefinery economics and highlight key cost and revenue drivers. Fig. 4 shows the annualized cost distribution, revenue-composition relationship, and phenol minimum selling price (MSP) for all forestry residue feedstocks. The MSP of phenol was used as the primary economic indicator, as phenol is the main target product of the RCF pathway. Revenues from co-products, including furfural and *p*-xylene, were incorporated as credits in the overall economic analysis. The phenol MSP, therefore, reflects the minimum price required for the entire system to achieve economic feasibility. Three major components dominated the total expenses for all feedstocks: purchased equipment, raw materials, and utilities. Their relative contributions changed slightly from case to case, with variations within 1-8% across all scenarios, indicating that the overall cost structure remained comparable among different biomass types. As lignin and total structural carbohydrate contents for each biomass fall within a ~10% range (55-65 wt% for lignin, 20-30 wt% for carbohydrates), the total amount of solvents, catalysts, and energy required in the RCF and MSH processes was similar, leading to comparable cost structures across forestry residues.

View Article Online
DOI: 10.1039/D6GC01047D

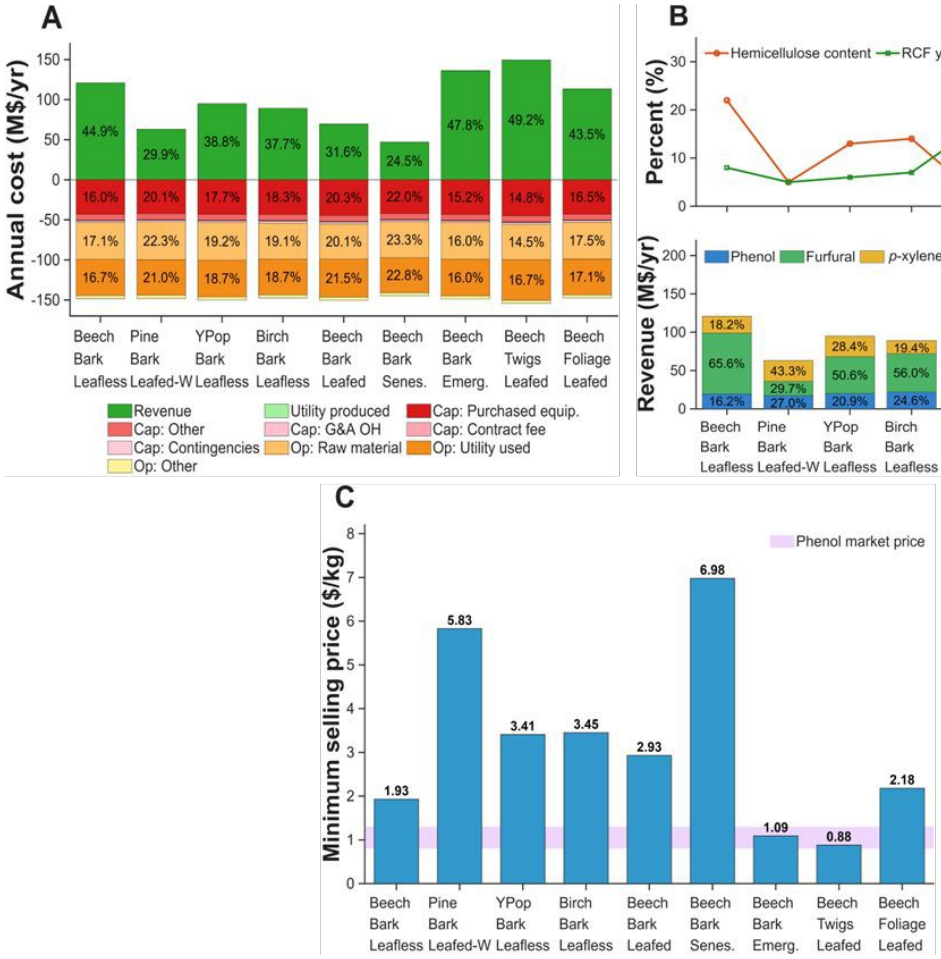

Fig. 4. TEA results for selected forestry residues. A) Annualized cost distribution, B) revenue distribution with hemicellulose content and RCF yield, and C) MSP of phenol for each biomass case. Cap is capital cost; Purchased equip. is purchased equipment cost; G&A OH is general and administrative overheads; Op is operating cost; and MSP is minimum selling price. The purple band represents the 2025 global phenol market price range.

Looking at the detailed cost breakdown, purchased equipment, raw materials, and utilities were the major process expenses. 85-90% of the purchased equipment expenses came from the RCF reactor for every case, primarily because of the high operating pressure of 80 bar. This finding agrees with literature that has also reported the RCF reactor as a dominant biorefinery expense.(21, 48) The dominant contributions to the raw material price were the pretreated biomass and LiBr, which accounted for around 50% and 30%, respectively. The pretreated biomass price included the expenses for harvesting, collecting, drying, and transportation – steps that are necessary to supply a process-ready feedstock. Among these, transportation and drying typically accounted for the largest portions of the overall biomass cost, 30-45% and 20-30%, respectively. The MSH process uses a 1:5

View Article Online
DOI: 10.1039/D6GC01047D

biomass-to-LiBr ratio by mass, so a large amount of LiBr is circulated through the process. Even though LiBr is recycled within the process, the combination of high unit price and high usage makes LiBr a key cost driver. Approximately 45% of the utility price came from steam, and about 30% came from hot oil, reflecting the strong thermal demand of the RCF-MSH system. Other utilities, such as electricity, cooling water, and refrigerant, contributed to much smaller fractions. The detailed capital and operating costs for all individual cases are in SI Section 4.

Unlike the cost segment, the annual revenue showed a much larger change between feedstocks, which was mainly governed by the hemicellulose content and the RCF yield (Fig. 4B) Hemicellulose is converted to furfural, which has a higher selling price ($1650/ton) in comparison to *p*-xylene ($1091/ton) and phenol ($1120/ton), so cases with higher hemicellulose fractions generated higher revenue. For instance, leafed American beech twigs/branchlets, emergence American beech bark, and leafless American beech bark contained relatively large hemicellulose fractions and consequently achieved higher annual revenues. In contrast, leafed American beech bark, senescence American beech bark, and leafed-W pitch pine bark contained less hemicellulose content and exhibited lower annual revenues. The RCF yield was the second most important factor for the revenue. Leafed American beech twigs/branchlets, which have both the highest hemicellulose content (30 wt%) and the highest RCF yield (18 wt%), achieved the largest revenue among all forestry residues. Leafed American beech bark had the lowest hemicellulose (3 wt%) and high lignin (64 wt%) content, but it had moderate revenue due to its relatively high RCF yield (16%). Conversely, senescence American beech bark had a composition similar to leafed American beech bark (4 wt% hemicellulose and 68 wt% lignin) but the lowest RCF yield (5%), leading to the lowest revenue. These trends demonstrate that, under similar cost structures, variations in hemicellulose content and RCF yield were the primary drivers of revenue and overall economic performance of the biorefinery process. Although uncertainty in these parameters may affect the absolute values of revenue or MSP, the relatively consistent cost structure across feedstocks and the dominant role of these variables in determining revenue suggest that the overall trends and ranking among feedstock scenarios remain robust.

In this study, three products (phenol, furfural, and *p*-xylene) were generated, but the economic comparison was focused on the RCF section by analyzing the results in terms of phenol MSP (Fig. 4C). The selling prices of furfural and *p*-xylene were fixed at their 2025 average market values, and the purple band in Fig. 4C indicates the current global phenol market price range in 2025 ($0.80-$1.30/kg).(49) When the MSP values were compared with this band, leafed American beech twigs/branchlets, emergence American beech bark, and leafless American beech bark emerged as the most promising cases. Leafed American beech twigs/branchlets had the lowest MSP ($0.88/kg), which is the most competitive with the current market range. This finding is consistent with the annual cost and revenue analysis results. For the American beech twigs/branchlets case, a sensitivity analysis was performed to examine how variations in key process and economic parameters influence the overall economic performance of the process. The RCF reactor pressure had the strongest effect on the phenol MSP (resulting in an MSP decrease to >$0.20/kg for a 16 bar reduction

View Article Online
DOI: 10.1039/D6GC01047D

in reactor pressure), mainly due to the sharp increase in reactor price at higher operating pressures. The furfural selling price was identified as the second most influential factor (resulting in an MSP reduction to >$0.40/kg for a $0.33/kg increase in selling price), reflecting its large contribution to the total revenue. The detailed sensitivity analysis results can be found in SI (Fig. S4).

Life cycle assessment

LCA provides a comprehensive system-level assessment by accounting for upstream and downstream impacts, including raw material production, utility consumption, transportation, process integration, co-product credits, and biogenic carbon effects. Herein, the global warming potential (GWP, expressed in kg of CO_2 equivalents (CO_2eq)) was evaluated using a functional unit of 1 metric ton of forest residues processed. As shown in Fig. 5, GWP values varied substantially depending on phenophase and tissue type, ranging from –380 kg CO_2eq for leafed American beech bark to –1540 kg CO_2eq for emergence American beech bark. Emissions were primarily driven by combustion and utility use, with smaller contributions from pretreatment and chemical inputs. These impacts were partially offset by mechanisms such as biogenic carbon uptake, on-site utility generation, and the avoided burden method that allocates environmental credits to co-products.(38)

Among the co-products, furfural contributed the largest GWP credit (–10.1 kg CO_2eq/kg furfural), followed by phenols (–3.5 kg CO_2eq/kg phenols) and *p*-xylene (–2.4 kg CO_2eq/kg *p*-xylene). Accordingly, scenarios with higher furfural yields (stemming from high hemicellulose contents) tended to have lower overall GWP, tracking with the trends in the economic analysis. GWP also varied across broader biological dimensions. Across species, for a fixed phenophase and plant constituent, GWP values ranged from –390 kg CO_2eq (pitch pine) to –1100 kg CO_2eq (American beech). Across phenophases, GWP ranged from –380 to –1540 kg CO_2eq, with leafed American beech bark the highest and emergence American beech bark the lowest. Across plant tissues, values spanned –380 to –1170 kg CO_2eq, with leafed American beech bark again showing the highest GWP and leafed American beech foliage the lowest. In previous work, the GWP was calculated for the bark, twigs, and foliage in the leafed phenophase for yellow poplar with values of –850, –1110, and –650 kg CO_2eq, respectively. Comparing these values to the current results for yellow poplar and American beech, the ranges are similar, with yellow poplar spanning –650 to –1110 kg CO_2eq and American beech spanning –380 to –1540 kg CO_2eq. This alignment is expected, as both are hardwood broadleaved species with comparable carbon compositions, although a more recent version of the Ecoinvent database was used in this study vs. the previous study.(50) Uncertainty in biomass composition and conversion yields will influence final product distributions, which in turn affect the calculated GWP results. Because multiple co-products contribute avoided-burden credits, changes in product distribution may alter the absolute magnitude of GWP without necessarily changing the broader comparative interpretation across feedstock scenarios. For all forestry residues considered, GWP was a net negative, highlighting that forestry residues are promising as sustainable biorefinery feedstocks. It is also worth noting that the utilities generated from the combustion exceed the utilities consumed in the process, and therefore each unit of energy produced provides a carbon offset. Together, these findings underscore the importance of considering species, phenophase, and plant tissue type in evaluating the climate impact of biomass utilization, as each factor contributes meaningfully to the overall GWP.

View Article Online
DOI: 10.1039/D6GC01047D

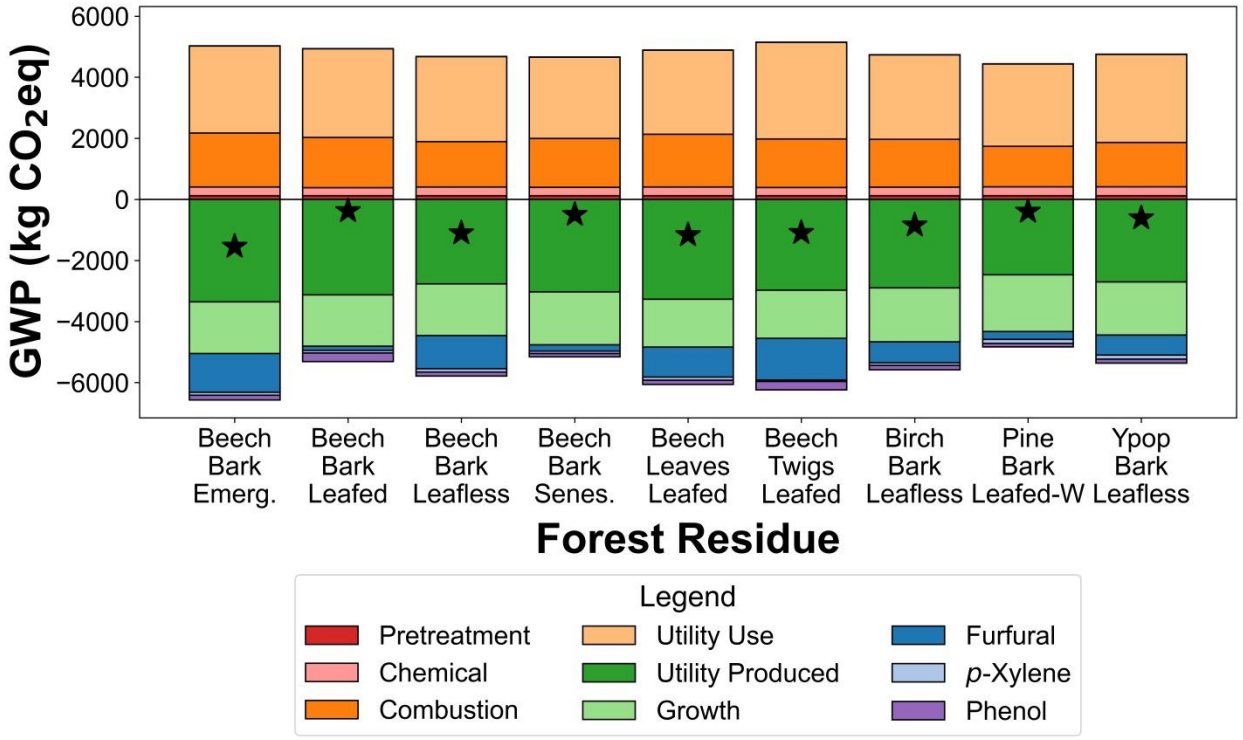

Fig. 5. GWP for 1 metric ton of forest residues processed. Bars represent contributions from individual process stages, including pretreatment, chemical conversion, combustion, utility use/production, and co-product allocation. Star markers (★) denote the net GWP.

Harvest optimization strategies and recommendations for future development

Together, the biomass characterization, TEA, and LCA can provide insights into harvest optimization strategies for forest residue biorefineries. Both the TEA and LCA identify hemicellulose as a critical driver for economics and sustainability, and our compositional analysis indicates that twigs/branchlets consistently have the highest xylan contents across species. Hardwood twigs also have significantly higher xylan values than softwood twigs, therefore making them a better biorefinery feedstock. Furthermore, RCF yield, which was determined to be highest in twigs/branchlets in the leafed/leafed-spring/summer (S) phenophase in previous work,(20) was identified as the second main driver for profitability. These findings indicate that hardwood twigs/branchlets in the leafed phenophase are the optimal forestry residue biofeedstock. This finding can also be used to screen other potential inputs that could be economically and environmentally viable using the metrics of high hemicellulose and RCF yields. For instance, grasses have the highest hemicellulose content compared to hardwoods and softwoods, and grassy energy crops and agricultural residues (*i.e.*, miscanthus, switchgrass, sorghum, corn stover) have significantly higher hemicellulose contents than tree biomass and would therefore likely produce significantly larger furfural yields.(51, 52) In another example, hybrid poplar has been genetically engineered to have improved RCF yields by reducing native interunit C-C bonds.(53) For such strategies to be feasible, higher-throughput characterization approaches that can screen for both RCF and hemicellulose yields will need to be adopted, such as a thermogravimetric analysis or fluorescence- screening approach,(54, 55) though future work is needed to further generalize these methods to additional

View Article Online
DOI: 10.1039/D6GC01047D

feedstock types. Furthermore, additional studies on combined biorefinery feedstocks are useful to further understand the impacts of mixed biomass biorefinery inputs and potentially optimize the process to practically handle mixed inputs while maximizing profitability and mitigating environmental impacts. The trends identified herein are evident in the four trees in this study that grow primarily in the Eastern temperate deciduous forest biome. Future work can determine if these trends can be extended more broadly to species in other geographic regions, climates, and conditions.(56, 57) Engagement with the timber industry could be valuable to determine a practical pathway to implement these harvest optimization approaches. The industrial implementation of these strategies depends on practical logistics, including the seasonality of site access and external factors such as extreme weather events.(7, 58) For instance, in colder regions, logging operations often halt in the winter, so strategies that target the leafless phenophase may not be feasible.(58) Beyond changing harvesting strategies, feedstock screening could be implemented to optimize biorefinery operations in the form of inventory management approaches, including tagging or sorting based on species/phenophase/residue type and long-term storage systems.(59, 60)

In addition to providing insight into feedstock selection, the TEA and LCA also highlighted areas for future biorefinery development. Understanding the impact of biofeedstock dynamics on biorefinery performance is crucial to inform process decisions, mitigate emissions, and maximize economic viability for commercial biorefineries. RCF pressure and cost were identified as key drivers of both biorefinery costs and the phenol MSP, owing to the high pressure needed during the reaction. Several studies have investigated strategies to lower RCF pressure, such as hydrogen-free RCF, which can achieve a significant reduction in reactor pressure and maintain high RCF yields.(61, 62) Hydrogen-free RCF using methanol (*i.e.,* the RCF solvent used in our process model) was shown to decrease the observed reactor pressure by ~20 bar, which is similar to the -20% variation modeled in the sensitivity analysis.(61) This reduction in the reactor pressure decreased the phenol MSP price to <$0.20/kg, which is at least 4x lower than the current global phenol market price, demonstrating the huge significance of reactor pressure reduction for the profitability of biorefineries. Under the conditions used in the current biorefinery model (*i.e.,* a Ru/C catalyst), a hydrogen-free RCF process would result in a slight decrease in phenolic yields, although other catalysts (*i.e.,* Pd/C, Pt/C) retain high yields under hydrogen-free RCF conditions.(62) Furthermore, there is the potential to reduce reactor pressure to well below 10 bar through the use of lower-vapor-pressure solvents, such as glycerol, the use of which enabled the development of an ambient-pressure, reactive-distillation RCF system.(61, 63) The relationship between RCF reactor cost and RCF reactor pressure between 10 and 80 bar is shown in Fig. S5, with reduction in pressure resulting in a nearly linear decrease in cost. Below 6-10 bar, however, there is anticipated to be a significant drop in reactor cost, as this is the limit at which a steel pressure vessel could be exchanged for a glass-lined reactor.(64-66) A previous TEA conducted for a traditional RCF system vs. an ambient pressure RCF system (enabled through the use of glycerin as the low-vapor-pressure solvent) demonstrated an ~2x reduction in capital costs, driven by the decrease in cost of the ambient pressure RCF reactor.(63) Although changing solvents likely affects phenolic product selectivities, and future studies are needed to determine the impact of varying phenolic selectivities on biorefinery economics and emissions, such studies show the high potential of lower-pressure RCF systems to drastically improve biorefinery economics.

The largest contributor to raw material costs is the LiBr salt used in the MSH process, even though it is largely recycled. Future research should investigate whether the LiBr inputs could be further

View Article Online
DOI: 10.1039/D6GC01047D

reduced while maintaining sugar yields, potentially through the inclusion of an additional catalyst.(25) Other salts, such as $ZnCl_2$, which has been used in a pilot-plant study of MSH,(67) also should be considered for the MSH process to determine whether costs can be reduced by using a less expensive or more efficient reagent. The other major raw material cost is the biomass feedstock itself, primarily due to transportation. This finding suggests that local feedstocks should be prioritized, which aligns with the conclusions in the literature that transportation costs are the major hurdle to the utilization of uncollected forestry residues.(11) The other major driver of feedstock cost is drying, and foliage tends to have the highest moisture content. Although the biomass was assumed to be air-dried in our process, other forms of drying (*i.e.,* kiln-drying) are extremely energy-intensive(68) – making foliage less preferable as a biorefinery feedstock in comparison to bark and twigs/branchlets. Finally, there is an opportunity to increase overall biorefinery economics by targeting higher-value bioproducts, such as phenolic-derived specialty materials, additives, flavors, fragrances, and pharmaceuticals.(34, 36, 37, 69)

Conclusions

Together, these results highlight the potential of forestry residues as promising profitable and sustainable biorefinery feedstocks. Directly connecting feedstock selection to biorefinery economics and environmental impacts highlighted that hemicellulose content and RCF yields strongly impact the biorefinery revenue and GWP. Hardwood twigs/branchlets in the leafed phenophase were identified as the optimal forestry residue biorefinery feedstock because of their high hemicellulose content and RCF yields, and other biomass with similar compositions are predicted to be promising biorefinery feedstocks. Major drivers of costs and CO_2 emissions also emphasize key areas for future biorefinery research, including RCF pressure reduction, LiBr concentrations and alternatives, and biofeedstock drying and transportation. This study demonstrates the critical role of feedstock selection in commercial biorefineries to inform process decisions, optimize valorization strategies, mitigate GHG emissions, and maximize economic feasibility. Overall, this work highlights the potential of forestry residues as profitable and sustainable biorefinery feedstocks to address the global environmental, social, and resource security concerns associated with our current fossil fuels-based economy.

View Article Online
DOI: 10.1039/D6GC01047D

Experimental

Sample collection

Forest residue samples were collected from within or near the Fair Hill Natural Resources Management Area, located in the northeastern corner of Cecil County, Maryland, U.S. (39°42′ N, 75°50′ W). Bark, twigs/branchlets, and foliage samples were collected from *P. rigida* Mill. (pitch pine), *L. tulipifera* L. (yellow poplar), *F. grandifolia* Ehrh. (American beech), and *B. lenta* L. (sweet birch), common tree species in the area, throughout the four phenophases. These species were chosen to include a range of traits, such as shade tolerance, crown structure, and bark thickness, which reflect their overall life strategies, and thus, their biomass compositions. Note that pitch pine, a softwood species that does not lose its foliage, experiences a leafed-W and leafed-S phenophases, in addition to emergence and senescence phenophases. For additional details, see previous work.(20)

Materials

Hexanes (98.5%) and calcium carbonate (ACS grade) were purchased from Fisher Scientific. Ethanol (200 proof, anhydrous) was purchased from Decon Laboratories. Sulfuric acid (72 % w/w) was purchased from Ricca Chemical. D-(+)-Xylose (>99%), 5-hydroxymethylfurfural (>99%), 2-furaldehyde (99%), and formic acid (>96%) were purchased from Sigma-Aldrich. D-(+)-glucose, (anhydrous, 99%) and levulinic acid (98%) were purchased from Alfa Aesar. A38S-500 acetic acid (glacial, ACS grade) was purchased from Fisher Chemical. All chemicals were used as received. No unexpected or unusually high safety hazards were encountered.

Biomass characterization

After collection, biomass samples were dried at 40 °C for 48 h, knife-milled, and sieved through a 2-mm screen. Extractives were removed according to literature procedures to reduce measurement interference.(4, 70) Briefly, samples were sonicated in ethanol (80 vol%) in deionized water at least four times, followed by sonication in hexanes at least twice until the solvent wash ran clear. Samples were subsequently dried under dynamic vacuum at 40 °C. Moisture content was determined *via* a Sartorius moisture content analyzer (MA 160). Structural carbohydrate compositions were measured using a National Renewable Energy Laboratory (NREL) procedure.(39) In this procedure, dried, extractive-free biomass underwent a two-step acid hydrolysis to fractionate the biomass and hydrolyze the sugars. The hydrolysate samples were analyzed on a Waters e2695 high-performance liquid chromatography (HPLC) instrument equipped with a Waters 2998 photodiode array detector (PDA) and Waters 2414 refractive index (RI) detector. The samples were filtered through 0.45-µm Nylon syringe filters prior to chromatographic analysis. A Bio-rad Aminex HPX-87H column was employed at a column oven temperature of 55 °C, with an aqueous solution of H_2SO_4 (0.005 M) as the mobile phase at a flow rate of 0.6 mL/min for detecting and quantifying glucose (9.2 min), xylose (9.8 min), acetic acid (15.0 min), levulinic acid (15.5 min), and formic acid (13.8 min) using the RI detector. HMF (29.12 min) and furfural (44.84 min) were also detected using the PDA detector at

View Article Online
DOI: 10.1039/D6GC01047D

254 nm. Standard compound calibration curves were used to quantify the concentrations. Total glucan and xylan contents were determined following literature.(29, 39)

It is worth noting that the NREL procedure has been extensively validated for woody samples but is generally considered more challenging for more complex samples, such as barks and leaves.(4) Other studies have used this method for forestry residues, enabling comparison with literature values.(71) The hemicellulose values reported are purely from the xylan content, which is anticipated to be the largest contributor to hemicellulose in these samples;(38) however, given the complex nature of these tissues, it is of interest for future research to study the dynamics of other hemicellulose components and confirm this assumption.

Process simulation

Process flowsheets in ASPEN Plus V12 simulated RCF, MSH, and STP processes as described in previous work.(38) Briefly, lignin was converted to phenolics *via* RCF, then the solid fraction was fed into an MSH process, in which the structural carbohydrate fraction was valorized to generate *p*-xylene and furfural. Finally, the unreacted solid waste and humins by-product was burned to produce both flue gas and excess utilities to generate additional energy. The numerical quantity of excess energy generation was calculated from the ASPEN flowsheet simulation and summed in MATLAB (2021a). Process input values for lignin, extractive, and ash content, and RCF yields were sourced from previous work.(20)

TEA modeling methodology

The economic assessment for chemical production was performed using Aspen Economic Analyzer V12. Discounted cash flow analysis and the production cost of chemicals were used to perform economic analysis for different cases. The MSP was selected as the economic indicator because it is widely used in process economics and enables direct and threshold-independent comparison of economic feasibility across multiple process scenarios under consistent assumptions. The MSP encompasses economic inputs and outputs to the biorefinery system, including feedstock and material costs, utilities, operating costs, capital costs, overheads, feeds, contingencies, and revenues. As the main product was phenols from the RCF process, the MSP of phenols at which the NPV becomes zero (*i.e.,* the break-even selling price) was used as the production cost of chemicals. To calculate the phenol MSP, the selling prices of furfural and *p*-xylene from the MSH process were fixed at \$1650/ton and \$1091/ton, respectively, corresponding to the 2025 global average market prices.(49) The additional assumptions used to perform the economic analysis are outlined below:

1. The analysis was conducted for a 20-year project lifetime with 8,000 operating hours per year, assuming a 10% interest rate, 21% corporate tax, and a 10% salvage value at the end of the project life.
2. All equipment and operating costs were directly obtained from the cost database built in Aspen Economic Analyzer V12, except for the RCF reactor. The RCF reactor was costed as a pressure vessel based on process specifications. The detailed cost estimation of the RCF reactor can be found in the SI.

View Article Online
DOI: 10.1039/D6GC01047D

3. The biomass feedstock price for each case was estimated using a heating-value-based approach, in which the cost of each biomass part (bark, twigs/branchlets, or foliage) was scaled in proportion to its lower heating value (LHV).(72) For reference, a price of $2/GJ and an LHV of 16.0 MJ/kg were used as the baseline, following the International Energy Agency's average for forest-residue wood chips.(73) Using this approach, the estimated prices ranged from $22/ton to $26/ton depending on species and energy content. The detailed heating value and the estimated biomass price of each case can be found in the SI.
4. The prices of other raw materials and chemicals were based on the previous study(74) and the 2025 global market averages(49) hexane: $687/ton, hydrogen: $653/ton, LiBr: $1400/ton, aluminum chloride: $600/ton, ethyl acetate: $910/ton, sulfuric acid: $123/ton, ethylene: $600/ton, and heptane: $1300/ton.

To ensure fair comparison across different biomass cases, the same financial and operational assumptions were maintained.

After analysis of the phenol MSP, a sensitivity analysis was performed for the most promising case, which exhibited the lowest phenol MSP. This analysis examined how variations in key process and economic parameters influenced the overall economic performance of the process. The parameters considered include the RCF reactor operating conditions, reactor capital cost, major material costs, and market prices of products. Each parameter was independently varied by ±20% relative to its base-case value, while keeping all other variables constant, to assess its impact on the calculated phenol MSP. The ±20% range was chosen because it is widely applied in TEA to represent practical levels of uncertainty in process design, capital estimation, and market prices. The results of this analysis provide valuable insight into the critical factors that should be prioritized for process optimization and cost reduction.

Additional details about the biomass price estimation, RCF reactor cost estimation, TEA, and sensitivity analysis can be found in SI Section 4 (Tables S7 and S8).

LCA modeling methodology

Goal and scope definition

This study represents a "cradle-to-gate" analysis of a biorefinery using American beech, pitch pine, sweet birch, and yellow poplar across plant tissues and phenophases as feedstocks to produce phenolics, *p*-xylene, and furfural. The analysis is intended to represent a U.S.-based biorefinery processing forest residues into valuable chemical products. A functional unit was chosen to be 1 metric ton of biomass feedstock, similar to previous analyses.(38, 75) This functional unit was selected because the system is a multiproduct biorefinery, and it enables all product outputs to be evaluated relative to a common biomass input basis.

View Article Online
DOI: 10.1039/D6GC01047D

Life cycle inventory

The life cycle inventory (LCI) was developed using Aspen Plus simulation results and data from Ecoinvent 3.3, with U.S.-specific regional data used when available, and global data used otherwise.(50) Mass and energy balances from the process simulations were used to quantify raw material and utilities requirements. The process design is based on RCF and MSH hydrolysis.

The system boundary includes all upstream and on-site operations, from biomass harvesting and preprocessing to final product output. Biomass pretreatment comprises activities such as collection, transportation, milling, chipping, pelleting, and drying prior to entering the RCF reactor. Following the methodology of Luo *et al.*, the upstream information regarding bark production was obtained from Ecoinvent, and twig/branchlet and foliage production used woodchip production as a surrogate from the Ecoinvent database.(38) A standard transportation distance of 112 km was assumed based on our previous work.(38) This assumption was applied uniformly across feedstock types because site-specific information on feedstock collection and transport was not available. The system boundary can be seen in Fig. S6.

Additional important assumptions for the LCA include the following:

1. The biorefinery was assumed to recycle nearly all cooling water, with only a 1% loss during standard operations.(74)
2. Contributions to GWP from facility infrastructure and catalysts were excluded, as buildings serve multiple functions and catalysts were considered long-lived during their operational lifespan.(74, 76)
3. The steam and power system was assumed to achieve complete combustion, emitting only CO_2 and water.(74)
4. Heat integration was conducted in Aspen Energy Analyzer to optimize utility use and improve energy efficiency.
5. Biogenic carbon uptake through photosynthesis was credited in the LCI, using species-specific carbon content to account for sequestration.(68, 75)
6. Direct land-use change and soil carbon effects were not included in this study.(77, 78) As the feedstock consists of forestry residues (*e.g.,* bark, twigs, and leaves from yellow poplar) rather than dedicated energy crops, these effects are less directly attributable to the biorefinery system and are highly site-specific.

These assumptions span both process-level modeling choices and LCA-specific scope definitions. Process assumptions, including cooling water recycling, complete combustion, and heat integration, determine the material and energy flows used to construct the life cycle inventory. By contrast, exclusions related to infrastructure, catalysts, and soil carbon effects define the boundaries of the environmental accounting. These exclusions may influence the absolute magnitude of GWP results and should therefore be considered as part of the study scope rather than as process-performance effects.

View Article Online
DOI: 10.1039/D6GC01047D

Life cycle impact assessment

The primary impact metric considered in this study was GWP, evaluated using the TRACI 2.1 impact assessment method.(79) Common co-product treatment methods include mass, economic, and avoided burden allocation. In this work, the avoided burden approach is applied to account for multiple co-products. Mass allocation was not chosen because product mass is not proportional to product value.(38) Economic allocation also was not chosen, as the commercial prices of several products, particularly phenolics and furfural, are not well established. In the avoided burden approach, the specific coproducts are electricity generation, *p*-xylene, phenol, and furfural production. This approach assigns credits for the products assumed to be displaced.

Interpretation

A contribution analysis was performed to identify the most significant drivers of GWP for each process. Additionally, a sensitivity analysis was conducted on the carbon content estimates to evaluate their influence on overall results. The purpose of this analysis was to identify the key contributors to GWP across species, phenophase, and plant tissue and to assess how these factors influence overall system performance.

For tabulated LCA inputs and outputs, carbon content estimations, and a sensitivity analysis on the carbon content estimates, see SI Section 5 (Tables S9-S18, Fig. S7).

Data analysis

General descriptive statistics, including maxima, minima, average, median, and standard deviation, were calculated for structural carbohydrate (xylan, glucan, total) concentrations on a phenophase, species, and component basis. The Shapiro-Wilk test for normality and Bartlett's test for homoscedasticity were conducted to determine whether parametric or non-parametric ANOVA should be employed. Based on these results, the appropriate one-way ANOVA was selected and used to identify significant differences (p-value < 0.05) among the four tree species. When the ANOVA test determined a significant finding among the four tree species, Dunn's method for multiple pairwise comparisons was employed to identify statistically significant differences between specific tree species. The analysis sequence also was performed for phenophase and component comparisons within the dataset. Statistical analyses were conducted in GraphPad Prism v. 10.5.

Acknowledgements

A.J.S., R.C.O., D.T., D.H., S.H., R.S., Y.G., S.G.H., S.S., D.G.V., M.I., D.F.L., and T.H.E. thank the National Science Foundation Growing Convergence Research program (NSF GCR CMMI 1934887) in Materials Life-Cycle Management for support of this work. R.M.O. and T.H.E. acknowledge financial support from the Center for Plastics Innovation, an Energy Frontier Research Center funded by the U.S. Department of Energy, Office of Science, Basic Energy Sciences, under award DE-SC0021166. The authors express their gratitude to the Fair Hill Natural Resources Management Area for permission to access the grounds for this study. The TOC was created with BioRender (https://biorender.com).

View Article Online
DOI: 10.1039/D6GC01047D

Author Contributions

Conceptualization: A.J.S., R.C.O., D.F.L., and T.H.E. Methodology: A.J.S., R.C.O., D.T., D.H., S.H., R.S., and S.S. Investigation and formal analysis: A.J.S., R.C.O., D.T., D.H., S.H., R.S., Y.G., S.G.H., and R.M.O. Writing (original draft): A.J.S., R.C.O., D.T., D.H., S.H., and R.S. Writing (review and editing): A.J.S., R.C.O., D.T., D.H., S.H., R.S., Y.G., S.G.H., Y.O., R.M.O., S.S., D.G.V., M.I., D.F.L., and T.H.E. Funding acquisition: D.G.V., D.F.L., and T.H.E. Supervision: D.G.V., M.I., D.F.L., and T.H.E. Project administration: T.H.E.

Conflicts of Interest

There are no conflicts to declare.

Data Availability

All data supporting the findings of this study are available within the article and its supplementary information (SI) or from the authors upon reasonable request.

View Article Online
DOI: 10.1039/D6GC01047D

References

1. Mendieta CM, Vallejos ME, Felissia FE, Chinga-Carrasco G, Area MC. Review: Bio-polyethylene from wood wastes. J Polym Environ. 2020;28(1):1-16.
2. Clark JH, Luque R, Matharu AS. Green chemistry, biofuels, and biorefinery. Annu Rev Chem Biomol Eng. 2012;3(1):183-207.
3. Zhou C-H, Xia X, Lin C-X, Tong D-S, Beltramini J. Catalytic conversion of lignocellulosic biomass to fine chemicals and fuels. Chem Soc Rev. 2011;40(11):5588-617.
4. Abu-Omar MM, Barta K, Beckham GT, Luterbacher JS, Ralph J, Rinaldi R, et al. Guidelines for performing lignin-first biorefining. Energy & Environmental Science. 2021;14(1):262-92.
5. Madadi M, Saleknezhad M, Hashemi SS, Kargaran E, Abbasi-Riyakhuni M, Cai D, et al. Sustainable poplar biorefinery producing butanol-rich solvents, furfural, and lignin-derived compounds with environmental and economic benefits. Biofuel Research Journal. 2025;12(4):2554-68.
6. Lee RA, Lavoie J-M. From first- to third-generation biofuels: Challenges of producing a commodity from a biomass of increasing complexity. Anim Front. 2013;3(2):6-11.
7. Shapiro AJ, O'Dea RM, Li SC, Ajah JC, Bass GF, Epps TH, III. Engineering innovations, challenges, and opportunities for lignocellulosic biorefineries: Leveraging biobased polymer production. Annu Rev Chem Biomol Eng. 2023;14(1):109-40.
8. Wang H, Bi X, Clift R. Utilization of forestry waste materials in British Columbia: Options and strategies. Renewable Sustainable Energy Rev. 2021;150:111480.
9. Titus BD, Brown K, Helmisaari H-S, Vanguelova E, Stupak I, Evans A, et al. Sustainable forest biomass: A review of current residue harvesting guidelines. Energy, Sustainability and Society. 2021;11:1-32.
10. Davis M, Lambert L, Jacobson R, Rossi D, Brandeis C, Fried J, et al. Chapter 4: Biomass from the forested land base. In: Langholtz MH, editor. 2023 Billion-Ton Report: An Assessment of US Renewable Carbon Resources. Oak Ridge, TN: Oak Ridge National Laboratory; 2024.
11. Bergman R, Berry M, Bilek EMT, Bowers T, Eastin I, Ganguly I, et al. Utilizing forest residues for the production of bioenergy and biobased products. Final Report: Biomass Research and Development Initiative Program Award Number DE-EE0006297. Washington, DC: U.S. Department of Energy.; 2018.
12. Klemm D, Heublein B, Fink H-P, Bohn A. Cellulose: Fascinating biopolymer and sustainable raw material. Angewandte Chemie International Edition. 2005;44(22):3358-93.
13. Schutyser W, Renders T, Bosch SVd, Koelewijn SF, Beckham GT, Sels BF. Chemicals from lignin: an interplay of lignocellulose fractionation, depolymerisation, and upgrading. Chem Soc Rev. 2018;47(3):852-908.
14. Dashek WV, Miglani GS. Plant Cells and Their Organelles. Chichester, WS: Wiley Blackwell; 2016.
15. Silveira RL, Stoyanov SR, Gusarov S, Skaf MS, Kovalenko A. Plant biomass recalcitrance: Effect of hemicellulose composition on nanoscale forces that control cell wall strength. Journal of the American Chemical Society. 2013;135(51):19048-51.
16. McCann MC, Carpita NC. Biomass recalcitrance: a multi-scale, multi-factor, and conversion-specific property. J Exp Bot. 2015;66(14):4109-18.
17. Levia DF, O'Halloran RC, Otsuka Y, Chang JL, Kaiser K, Nanko K, et al. Stemflow unveils trees' weatherproofing stratagem during autumnal senescence. Plant, Cell & Environment. 2025;48(9):7001-4.

View Article Online
DOI: 10.1039/D6GC01047D

18. Baïer M, Goldberg R, Catesson A-M, Liberman M, Bouchemal N, Michon V, du Penhoat CH. Pectin changes in samples containing poplar cambium and inner bark in relation to the seasonal cycle. Planta. 1994;193(3):446-54.
19. Eberhardt TL, Samuelson LJ. Comparison of lignin and polysaccharide sugar contents for slash, longleaf, and loblolly pine growth rings formed during periods of soil moisture extremes. Wood Science and Technology. 2022;56:389-408.
20. O'Halloran RC, Shapiro AJ, Gupta Y, Long A, Haney SG, Otsuka Y, et al. Following forest cues for the harvest optimization of tomorrow's biofeedstocks. Green Chem. 2026;28:827-38.
21. Bartling AW, Stone ML, Hanes RJ, Bhatt A, Zhang Y, Biddy MJ, et al. Techno-economic analysis and life cycle assessment of a biorefinery utilizing reductive catalytic fractionation. Energy & Environmental Science. 2021;14(8):4147-68.
22. Davis R, Tao L, Tan ECD, Biddy MJ, Beckham GT, Scarlata C, et al. Process design and economics for the conversion of lignocellulosic biomass to hydrocarbons: Dilute-acid and enzymatic deconstruction of biomass to sugars and biological conversion of sugars to hydrocarbons. United States: National Renewable Energy Lab. (NREL), Golden, CO (United States); 2013. Contract No.: NREL/TP-5100-60223.
23. Corona A, Biddy MJ, Vardon DR, Birkved M, Hauschild MZ, Beckham GT. Life cycle assessment of adipic acid production from lignin. Green Chem. 2018;20(16):3857-66.
24. Sadula S, Oesterling O, Nardone A, Dinkelacker B, Saha B. One-pot integrated processing of biopolymers to furfurals in molten salt hydrate: understanding synergy in acidity. Green Chem. 2017;19(16):3888-98.
25. Freitas Paiva M, Sadula S, Vlachos DG, Wojcieszak R, Vanhove G, Bellot Noronha F. Advancing lignocellulosic biomass fractionation through molten salt hydrates: Catalyst-enhanced pretreatment for sustainable biorefineries. ChemSusChem. 2024;17(22):e202400396.
26. Deng W, Kennedy JR, Tsilomelekis G, Zheng W, Nikolakis V. Cellulose hydrolysis in acidified LiBr molten salt hydrate media. Ind Eng Chem Res. 2015;54(19):5226-36.
27. Liu Q, Luo S, Fan W, Ouyang X, Qiu X. Separation of short-chain glucan oligomers from molten salt hydrate and hydrolysis to glucose. Green Chem. 2021;23(11):4114-24.
28. Sadula S, Quiroz NR, Athaley A, Osamudiamhen Ebikade E, Ierapetritou M, G. Vlachos D, Saha B. One-step lignocellulose depolymerization and saccharification to high sugar yield and less condensed isolated lignin. Green Chem. 2021;23(3):1200-11.
29. Sadula S, Athaley A, Zheng W, Ierapetritou M, Saha B. Process intensification for cellulosic biorefineries. ChemSusChem. 2017;10(12):2566-72.
30. Grand View Research. *Paraxylene Market (2025-2030)*. 2025. https://www.grandviewresearch.com/industry-analysis/paraxylene-market (accessed 11/20/25).
31. Business analytiq. *Furfural Price Index*. 2025. https://businessanalytiq.com/procurementanalytics/index/furfural-price-index/ (accessed 3/27/25).
32. Zion Market Research. *Bio-based Paraxylene Market*. 2025. https://www.zionmarketresearch.com/report/bio-based-paraxylene-market (accessed 3/27/25).
33. Ebikade EO, Sadula S, Liu S, Vlachos DG. Lignin monomer conversion into biolubricant base oils. Green Chem. 2021;23(24):10090-100.
34. Wang S, Shuai L, Saha B, Vlachos DG, Epps TH, III. From tree to tape: Direct synthesis of pressure sensitive adhesives from depolymerized raw lignocellulosic biomass. ACS Cent Sci. 2018;4(6):701-8.

View Article Online
DOI: 10.1039/D6GC01047D

35. Mahajan JS, Hinton ZR, Nombera Bueno E, Epps TH, III, Korley LTJ. Lignin-derivable, thermoplastic, non-isocyanate polyurethanes with increased hydrogen-bonding content and toughness vs. petroleum-derived analogues. Materials Advances. 2024;5(9):3950-64.
36. Karagoz P, Khiawjan S, Marques MPC, Santzouk S, Bugg TDH, Lye GJ. Pharmaceutical applications of lignin-derived chemicals and lignin-based materials: linking lignin source and processing with clinical indication. Biomass Conversion and Biorefinery. 2024;14(21):26553-74.
37. Borregaard. *Borregaard - The Sustainable Biorefinery*. 2025. https://www.borregaard.com/ (accessed 1/8/26).
38. Luo Y, O'Dea RM, Gupta Y, Chang J, Sadula S, Soh LP, et al. A life cycle greenhouse gas model of a yellow poplar forest residue reductive catalytic fractionation biorefinery. Environ Eng Sci. 2022;39(10):821-33.
39. Sluiter JB, Ruiz RO, Scarlata CJ, Sluiter AD, Templeton DW. Compositional analysis of lignocellulosic feedstocks. 1. Review and description of methods. J Agric Food Chem. 2010;58(16):9043-53.
40. Ajao O, Benali M, Faye A, Li H, Maillard D, Ton-That MT. Multi-product biorefinery system for wood-barks valorization into tannins extracts, lignin-based polyurethane foam and cellulose-based composites: Techno-economic evaluation. Industrial Crops and Products. 2021;167:113435.
41. Johansson MB. The chemical composition of needle and leaf litter from Scots pine, Norway spruce and white birch in Scandinavian forests. Forestry. 1995;68(1):49-62.
42. Xiao M-Z, Chen W-J, Hong S, Pang B, Cao X-F, Wang Y-Y, et al. Structural characterization of lignin in heartwood, sapwood, and bark of eucalyptus. Int J Biol Macromol. 2019;138:519-27.
43. Neiva DM, Rencoret J, Marques G, Gutiérrez A, Gominho J, Pereira H, del Río JC. Lignin from tree barks: Chemical structure and valorization. ChemSusChem. 2020;13(17):4537-47.
44. Yoshimi Y, Tryfona T, Dupree P. Structure, modification pattern, and conformation of hemicellulose in plant biomass. Journal of Applied Glycoscience. 2024;72(1).
45. Kofujita H, Ettyu K, Ota M. Characterization of the major components in bark from five Japanese tree species for chemical utilization. Wood Science and Technology. 1999;33(3):223-8.
46. Sariyildiz T, Anderson JM. Variation in the chemical composition of green leaves and leaf litters from three deciduous tree species growing on different soil types. Forest Ecology and Management. 2005;210(1):303-19.
47. Borovkova VS, Malyar YN, Sudakova IG, Chudina AI, Zimonin DV, Skripnikov AM, et al. Composition and structure of aspen (Pópulus trémula) hemicelluloses obtained by oxidative delignification. Polymers. 2022;14(21):4521.
48. Madadi M, Kargaran E, Hashemi SS, Sun C, Denayer JFM, Karimi K, et al. Scalable Lignin Monomer Production Via Machine Learning-Guided Reductive Catalytic Fractionation of Lignocellulose. Advanced Science. 2025;12(42):e10496.
49. IMARC Group. *Chemicals and Materials Market Research Reports*. 2025. https://www.imarcgroup.com/categories/chemicals-market-reports (accessed 11/11/25).
50. Wernet G, Bauer C, Steubing B, Reinhard J, Moreno-Ruiz E, Weidema B. The ecoinvent database version 3 (part I): overview and methodology. The International Journal of Life Cycle Assessment. 2016;21(9):1218-30.

View Article Online
DOI: 10.1039/D6GC01047D

51. Segers B, Nimmegeers P, Spiller M, Tofani G, Jasiukaitytė-Grojzdek E, Dace E, et al. Lignocellulosic biomass valorisation: a review of feedstocks, processes and potential value chains and their implications for the decision-making process. RSC Sustainability. 2024;2(12):3730-49.
52. U.S. Department of Energy INL. *Bioenergy Feedstock Library*. 2023. bioenergylibrary.inl.gov (accessed 5/5/23).
53. Shuai L, Amiri MT, Questell-Santiago YM, Héroguel F, Li Y, Kim H, et al. Formaldehyde stabilization facilitates lignin monomer production during biomass depolymerization. Science. 2016;354(6310):329-33.
54. Shapiro AJ, O'Dea RM, Epps TH, III. Thermogravimetric analysis as a high-throughput lignocellulosic biomass characterization method. ACS Sustainable Chem Eng. 2023;11(49):17216-23.
55. O'Halloran RC, Shapiro AJ, Gupta Y, Guerard JJ, Siple D, Sadula S, et al. Stemflow fluorescence predicts lignin composition and phenolic monomer yield for trees. ACS Sustainable Chem Eng. 2025;13(24):9063-73.
56. Kelly SM, Munoz-Munoz J, van Sinderen D. Plant glycan metabolism by Bifidobacteria. Frontiers in Microbiology. 2021;Volume 12 - 2021.
57. Alberts B, Johnson A, Lewis J, Raff M, Roberts K, Walter P. Molecular Biology of the Cell. 4th ed. New York: Garland Science; 2002.
58. Berry MD, Sessions J. A forest-to-product biomass supply chain in the Pacific Northwest, USA: A multi-product approach. Applied Engineering in Agriculture. 2018;34(1):109-24.
59. Kenney KL, Smith WA, Gresham GL, Westover TL. Understanding biomass feedstock variability. Biofuels. 2013;4(1):111-27.
60. Kizha AR, Han H-S. Processing and sorting forest residues: Cost, productivity and managerial impacts. Biomass Bioenergy. 2016;93:97-106.
61. Facas GG, Brandner DG, Bussard JR, Román-Leshkov Y, Beckham GT. Interdependence of solvent and catalyst selection on low pressure hydrogen-free reductive catalytic fractionation. ACS Sustainable Chem Eng. 2023;11(12):4517-22.
62. Kenny JK, Brandner DG, Neefe SR, Michener WE, Román-Leshkov Y, Beckham GT, Medlin JW. Catalyst choice impacts aromatic monomer yields and selectivity in hydrogen-free reductive catalytic fractionation. Reaction Chemistry & Engineering. 2022;7(12):2527-33.
63. O'Dea RM, Pranda PA, Luo Y, Amitrano A, Ebikade EO, Gottlieb ER, et al. Ambient-pressure lignin valorization to high-performance polymers by intensified reductive catalytic deconstruction. Sci Adv. 2022;8(3):eabj7523.
64. Parr Instrument Company. *https://www.parrinst.com/glass-reactors/*. 2026. (accessed 4/24/26).
65. Mayo J. *Designing a Glass-Lined Vessel: How to Specify a Reactor [Part 1]*. 2025. https://www.ddpsinc.com/blog/designing-a-glass-lined-reactor-a-practical-overview-on-specifying-a-reactor-part-1 (accessed 4/24/26).
66. Pfaudler. DIN BE Reactors. 2026. Contract No.: 624-13 E I 03/2026.
67. Van den Bergh J, Babich IV, O'Connor P, Moulijn JA. Production of monosugars from lignocellulosic biomass in molten salt hydrates: Process design and techno-economic analysis. Ind Eng Chem Res. 2017;56(45):13423-33.
68. Sahoo K, Bergman R, Runge T. Life-cycle assessment of redwood lumber products in the US. The International Journal of Life Cycle Assessment. 2021;26(8):1702-20.
69. Cywar RM, Rorrer NA, Hoyt CB, Beckham GT, Chen EYX. Bio-based polymers with performance-advantaged properties. Nat Rev Mater. 2022;7(2):83-103.

View Article Online
DOI: 10.1039/D6GC01047D

70. Theander O. Chemical analysis of lignocellulose materials. Animal Feed Science and Technology. 1991;32(1):35-44.
71. Hatfield R, Fukushima RS. Can lignin be accurately measured? Crop Science. 2005;45(3):832-9.
72. International Energy Agency. Good Practice Guidelines Biorefinery Project Development and Biomass Supply. Paris, France; 2007.
73. Labriet M. Biomass Production and Logistics. IEA Energy Technology Network; 2013.
74. Athaley A, Annam P, Saha B, Ierapetritou M. Techno-economic and life cycle analysis of different types of hydrolysis process for the production of p-Xylene. Comput Chem Eng. 2019;121:685-95.
75. Calicioglu O, Femeena PV, Mutel CL, Sills DL, Richard TL, Brennan RA. Techno-economic analysis and life cycle assessment of an integrated wastewater-derived duckweed biorefinery. ACS Sustainable Chem Eng. 2021;9(28):9395-408.
76. Benavides PT, Cronauer DC, Adom F, Wang Z, Dunn JB. The influence of catalysts on biofuel life cycle analysis (LCA). Sustainable Materials and Technologies. 2017;11:53-9.
77. Havlík P, Schneider UA, Schmid E, Böttcher H, Fritz S, Skalský R, et al. Global land-use implications of first and second generation biofuel targets. Energy Policy. 2011;39(10):5690-702.
78. Wong A, Zhang H, Kumar A. Life cycle assessment of renewable diesel production from lignocellulosic biomass. The International Journal of Life Cycle Assessment. 2016;21(10):1404-24.
79. Bare J. TRACI 2.0: the tool for the reduction and assessment of chemical and other environmental impacts 2.0. Clean Technologies and Environmental Policy. 2011;13(5):687-96.

View Article Online
DOI: 10.1039/D6GC01047D

Data Availability

All data supporting the findings of this study are available within the article and its supplementary information (SI) or from the authors upon reasonable request.